Supplementary Information

Novel Stable Metal-Organic Framework Photocatalyst for Light-Driven Hydrogen Production

Qi Yu,† Hong Dong,† Xin Zhang,† Ya-Xin Zhu, Jian-Hui Wang, Feng-Ming Zhang* and Xiao-Jun Sun*

School of Materials Science and Engineering, College of Chemical and Environmental Engineering, Harbin University of Science and Technology, Harbin,150040, P. R. China.

† Qi Yu, Hong Dong and Xin Zhang contributed equally to this work and should be considered co-first authors.

*E-mail: zhangfm80@163.com

*E-mail: sunxiaojun@hrbust.edu.cn

Contents

Materials and Characterization

DMF, EtOH were purchased from Tianjing zhiyuan chemical reagent Co.,Ltd. (Tianjing, China) $Dy(NO_3)_3 \cdot 6H_2O$ and 5-aminoisophthalic acid were obtained from Aladdin, Jianglai and Aldrich. NaOH, Na_2SO_4 was purchased from Hubei Yuancheng Company, (Hubei, China). All solvents and reagents were analytical grade and used without further purification.

Infrared spectrum using the KBr pellet was measured on a Bruker Tensor 27 in the range of 4000-400 cm^{-1}. Thermogravimetric (TG) analysis was carried out on a Netzch STA449F3 analyser at a heating rate of 10 °C/min from ambient temperature to 750 °C. X-ray powder diffraction (PXRD) patterns were recorded on a DX-2700B X-ray diffractmeter. The patterns were collected at a scanning rate of 5° per min in the 2θ range from 5-50°. Cyclic voltammograms (CV) were easured with a CHI760D workstation in a conventional three lectrode system with a scanning rate of 50 mV s^{-1}. A carbon-paste orking electrode, a Pt counter electrode and an Ag/AgCl reference lectrode were used. Measurements were performed in a 1 M Na_2SO_4 solution. Diffuse eflectance UV-vis spectra was carried out with a Lambda 35 spectrometer.

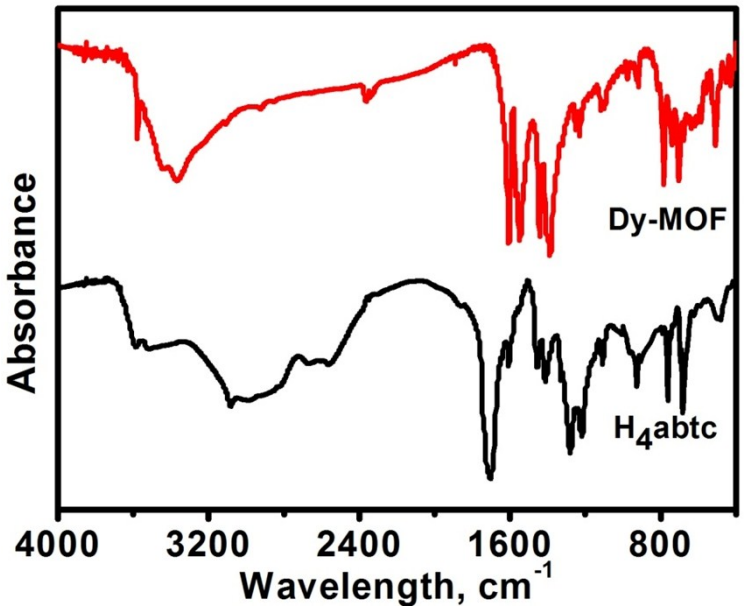

Figure S1. FT-IR spectra of dye-based Dy-MOF and H_4abtc ligand.

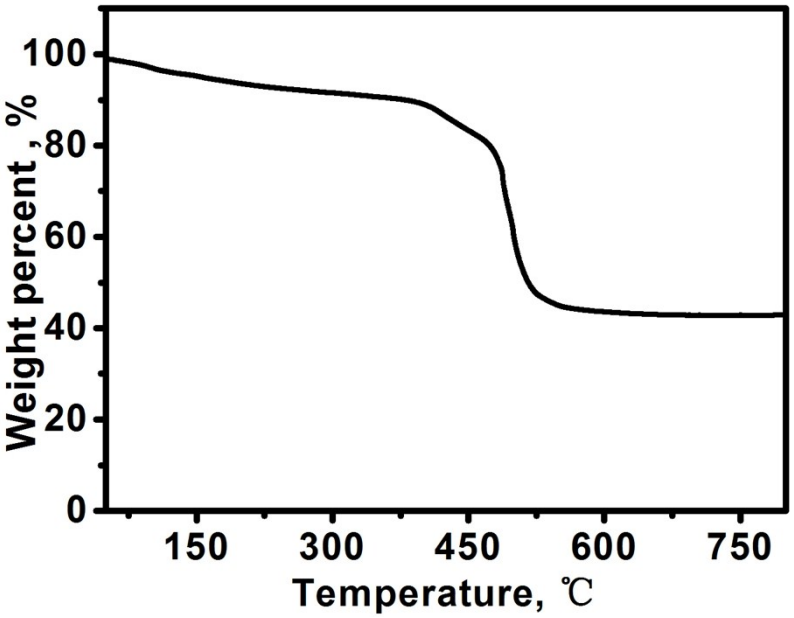

Figure S2. TGA curve of dye-basedz Dy-MOF.

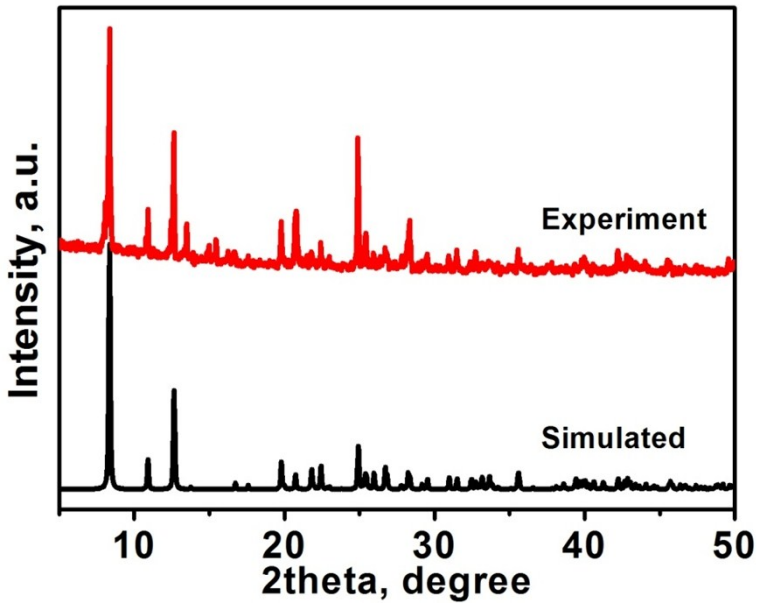

Figure S3. XRD datas of dye-based Dy-MOF for the simulated pattern and as-synthesized sample.

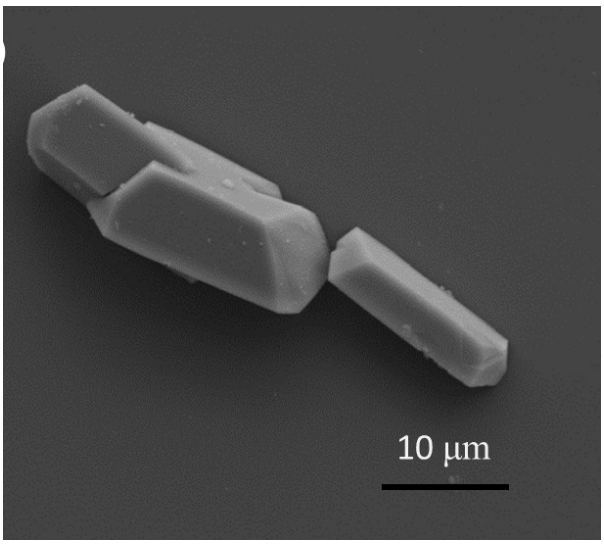

Figure S4. SEM image of dye-based Dy-MOF.

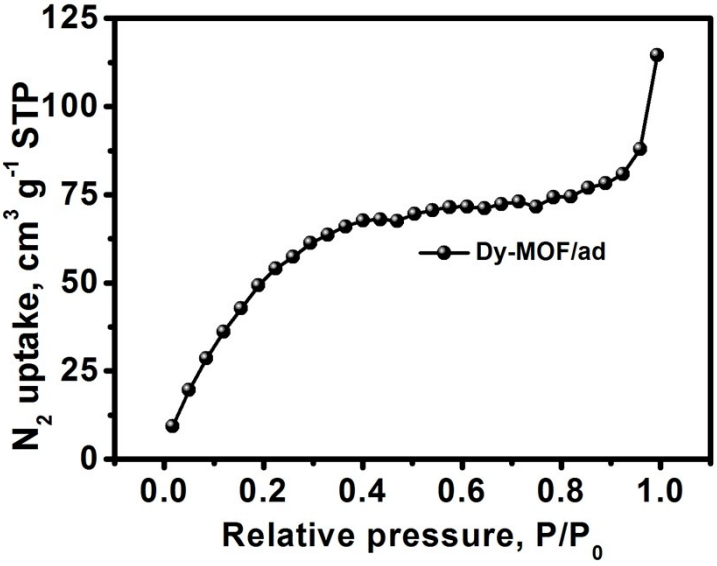

Figure S5. N_2 adsorption isotherms of dye-based Dy-MOF.

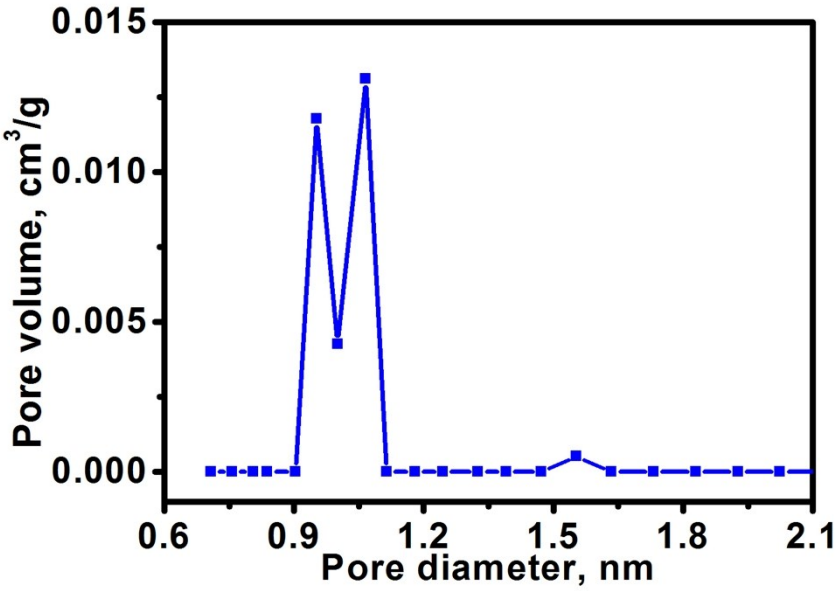

Figure S6. Pore size distribution of dye-based Dy-MOF.

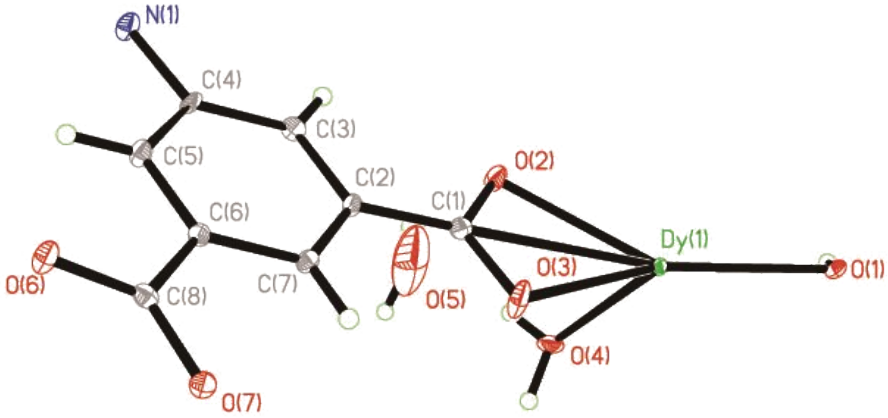

Figure S7. The least asymmetric unit of dye-based Dy-MOF.

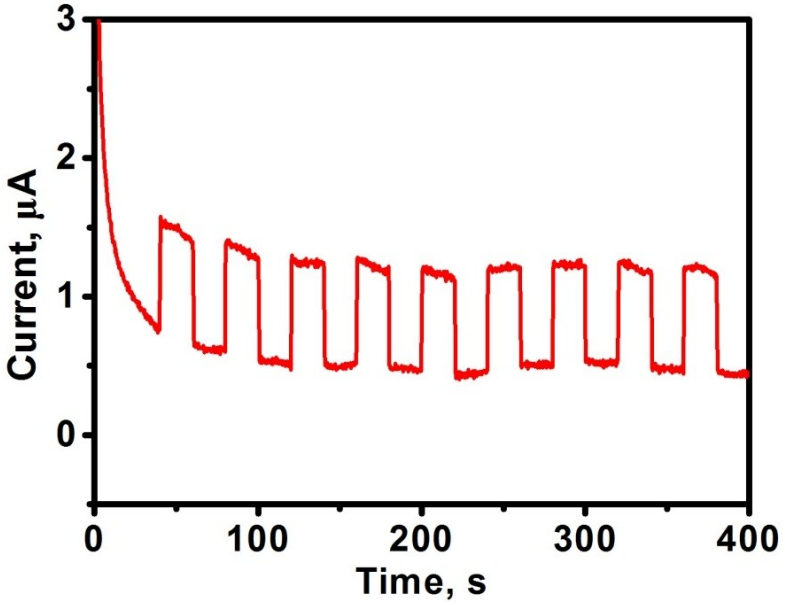

Figure S8. Photocurrent response curve of dye-based Dy-MOF.

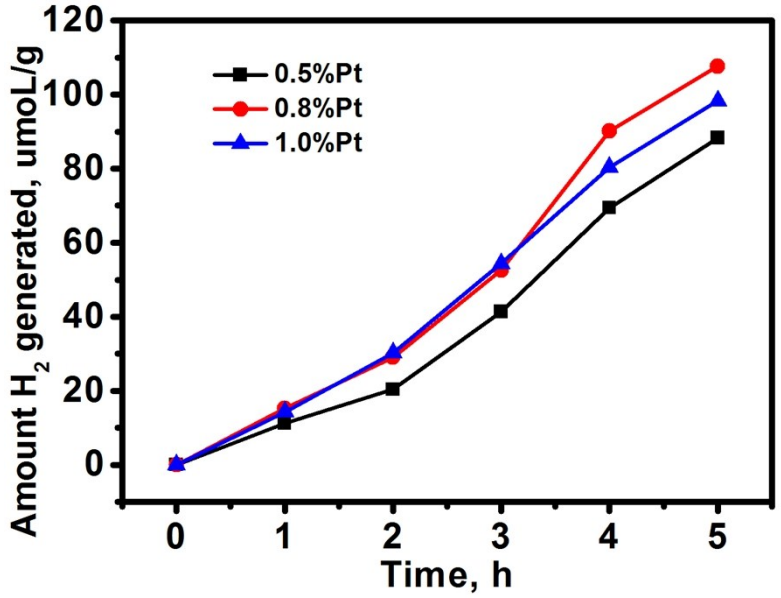

Figure S9. Photocatalytic H_2 generation rates for dye-based Dy-MOF (0.5, 0.8 and 1.0 wt % Pt).

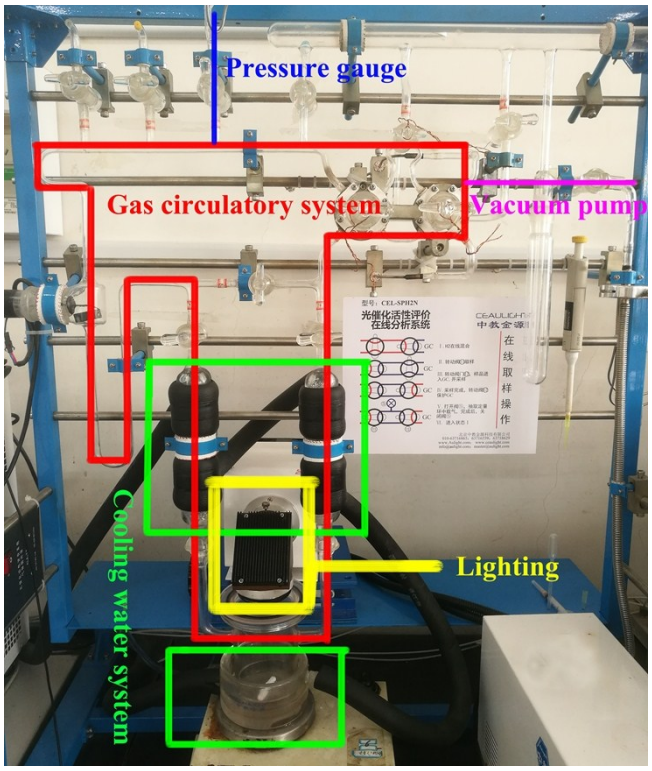

Figure S10. The photocatalytic H_2 production activity evaluation system.

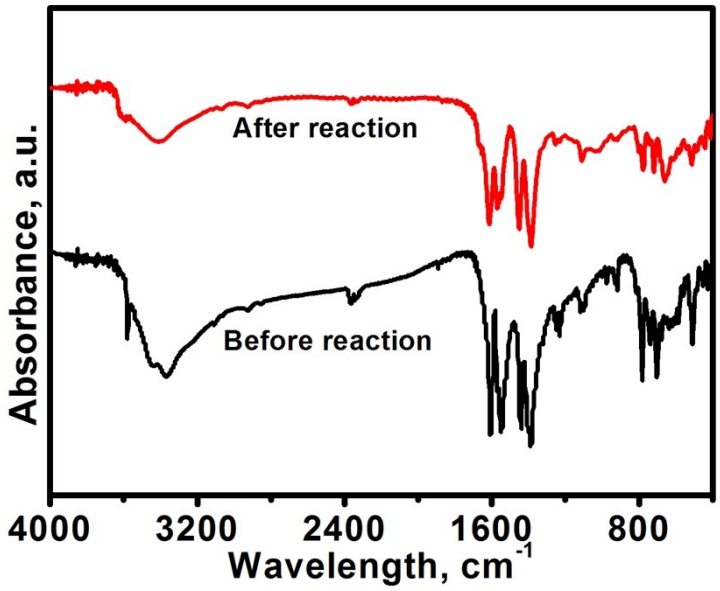

Figure S11. FT-IR spectra of dye-based Dy-MOF after and before reaction.

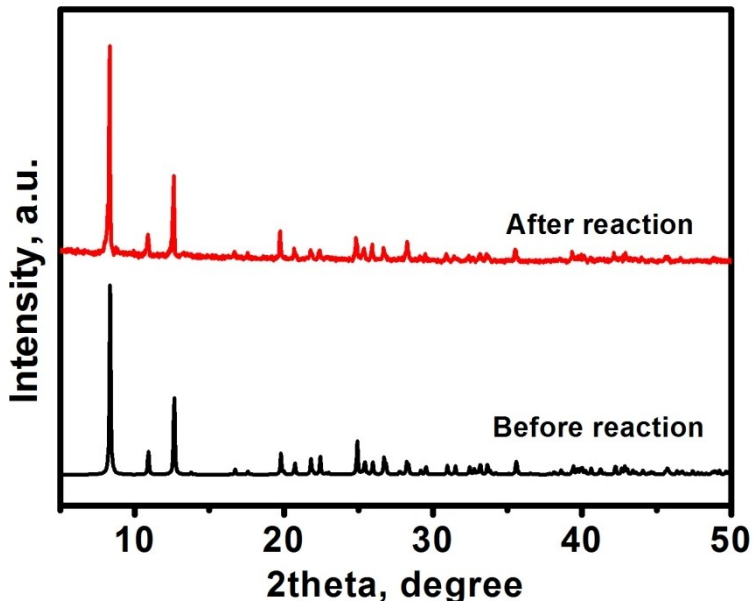

Figure S12. The XRD datas of dye-based Dy-MOF after and before reaction.

Figure S13. The dye-based Dy-MOF samples of after reaction and before reaction.

Table S1. Crystal data and structure refinement for dye-based Dy−MOF

Compound	**Dy−MOF**
formula	$C_8H_9O_7Dy$
fw	390.08
crystal system	Monoclinic
space group	P 21/n
a (Å)	4.55760(10)
b (Å)	16.2048(4)
c (Å)	14.0456(3)
α (deg)	90
β (deg)	95.241(2)
γ (deg)	90
V (Å^3)	1033.00(4)
Z	4
D_{calcd} (g cm^{-3})	2.508
R(int)	293(2)
μ (mm^{-1})	6.871
F (000)	740
R_1 [$I > 2\sigma(I)$]^a	0.0213
wR_2 [$I > 2\sigma(I)$]^b	0.0436
R_1 (all data)	0.0276
wR_2 (all date)	0.0456
GOF on F^2	1.034

$^a R_1 = \sum||F_o| - |F_c||/|F_o|$. $^b wR_2 = [\sum w (F_o^2 - F_c^2)^2/\sum w(F_o^2)^2]^{1/2}$.

Table S2. Selected bond lengths (Å) and angles (deg) for dye-based Dy−MOF

Dy(1)-O(3)#6	2.301(3)	Dy(1)-O(4)#7	2.364(3)
Dy(1)-O(6)#4	2.393(3)	Dy(1)-O(6)#5	2.403(3)
Dy(1)#4-O(6)-Dy(1)	104.01(10)	Dy(1)#4-O(6)-Dy(1)#5	143.70(13)
Dy(1)-O(6)-Dy(1)#5	100.42(10)	O(3)#6-Dy(1)-O(5)	73.18(10)
O(3)#6-Dy(1)-O(4)#7	143.32(9)	O(5)-Dy(1)-O(4)#7	141.20(10)
O(3)#6-Dy(1)-O(6)#4	120.11(10)	O(5)-Dy(1)-O(6)#4	76.27(10)
O(4)#7-Dy(1)-O(6)#4	72.14(10)	O(3)#6-Dy(1)-O(6)	74.93(9)
O(5)-Dy(1)-O(6)	117.92(10)	O(4)#7-Dy(1)-O(6)	75.45(9)
O(6)#4-Dy(1)-O(6)	75.99(10)	O(3)#6-Dy(1)-O(6)#5	77.79(10)
O(5)-Dy(1)-O(6)#5	139.65(10)	O(4)#7-Dy(1)-O(6)#5	76.01(9)
O(6)#4-Dy(1)-O(6)#5	143.70(13)	O(6)-Dy(1)-O(6)#5	79.58(10)
O(3)#6-Dy(1)-O(1)	135.52(10)	O(5)-Dy(1)-O(1)	83.03(11)
O(4)#7-Dy(1)-O(2)	114.76(10)	O(6)#4-Dy(1)-O(2)	132.27(10)
O(6)-Dy(1)-O(2)	151.19(9)	O(6)#5-Dy(1)-O(2)	77.31(10)
O(1)-Dy(1)-O(2)	53.21(9)		

Symmetry transformations used to generate equivalent atoms: #1 = − y + 1/3, − x + 2/3, z + 1/6, #2 = y, − x + y, − z; #3 = − x + y + 1/3, y − 1/3, z + 1/6; #4 = y + 1/3, x − 1/3, − z + 1/6; #5 = − x + 1, − y, −z; #6 = − y + 2/3, − x + 1/3, z − 1/6; #7 = x − y, x, −z; #8 = − x + y + 2/3,

y + 1/3,